Persistent changes in the intrinsic excitability of rat deep cerebellar nuclear neurones induced by EPSP or IPSP bursts

Wei Zhang, Jung Hoon Shin and David J. Linden

Department of Neuroscience, The Johns Hopkins University School of Medicine, 725 N. Wolfe Street, 916 Hunterian Building, Baltimore, MD 21205, USA

The deep cerebellar nuclei (DCN) are the major output of the cerebellum, and have been proposed as a site of memory storage for certain forms of motor learning. Microelectrode and whole-cell patch recordings were performed on DCN neurones in acute slices of juvenile rat cerebellum. DCN neurones display tonic and bursting basal firing patterns. In tonically firing neurones, a stimulus consisting of EPSP bursts produced a brief increase in dendritic Ca^{2+} concentration and a persistent increase in the number of spikes elicited by a depolarizing test pulse, along with a decrease in spike threshold. In intrinsically bursting DCN neurones, EPSP bursts induced an increase in the number of depolarization-evoked spikes in some neurones, but in others produced a change to a more tonic firing pattern. Application of IPSP bursts evoked a large number of rebound spikes and an associated dendritic Ca^{2+} transient, which also produced a persistent increase in the number of spikes elicited by a test pulse. Intracellular perfusion of the Ca^{2+} chelator BAPTA prevented the increase in intrinsic excitability. Thus, rapid changes in intrinsic excitability in the DCN may be driven by bursts of both EPSPs and IPSPs, and may result in persistent changes to both firing frequency and pattern.

(Resubmitted 12 July 2004; accepted after revision 18 October 2004; first published online 21 October 2004)
Corresponding author D. J. Linden: Department of Neuroscience, The Johns Hopkins University School of Medicine, 725 N. Wolfe Street, 916 Hunterian Building, Baltimore, MD 21205, USA. Email: dlinden@jhmi.edu

The cerebellum has a central function in sensorimotor integration and learning. The neurones of the deep cerebellar nuclei (DCN) comprise the main output stage of the cerebellum through their projections to premotor centres and the inferior olive. The DCN neurones receive GABAergic inhibitory drive from Purkinje cells in the cerebellar cortex, and glutamatergic excitatory drive from climbing fibre collaterals (which also innervate Purkinje cells) and mossy fibre collaterals (which also innervate granule cells). The granule cells elaborate axons which provide glutamatergic drive to the cerebellar cortex including the Purkinje cells and cortical interneurones. The Purkinje cell projection to the DCN (or its cognate structure, the vestibular nuclei) comprises the sole output of the cerebellar cortex. It completes the cerebellar cortical processing loop and conveys the integration and computation performed by the cortical circuit to the DCN.

DCN neurones *in vivo* typically fire spontaneously at 10–20 Hz (Thach, 1968; McDevitt *et al.* 1987; LeDoux *et al.* 1998). Artificial injection of depolarizing current can increase this firing frequency up to 300 Hz (Jahnsen, 1986). DCN neurones also show rebound excitation following a burst of IPSPs or injection of hyperpolarizing current. Repolarization is often accompanied by a 'rebound' depolarizing envelope (driven by I_h, a persistent Na^+ conductance and low-threshold Ca^{2+} current) which triggers Na^+ spike firing (Jahnsen, 1986; Llinas & Muhlethaler, 1988; Aizenman & Linden, 1999; Raman *et al.* 2000). The rebound depolarization is terminated in part by the opening of SK-type Ca^{2+}-sensitive K^+ channels (Aizenman & Linden, 1999). Thus, DCN neurones can respond to either the onset of EPSP bursts or the offset of IPSP bursts with transient increases in firing rate.

Several lines of evidence have implicated the DCN in the storage of certain forms of motor learning, particularly associative eyelid conditioning. Extracellular recordings made from behaving rabbits have shown that DCN neurones (particularly those in the interposed nucleus) reflect the memory trace for associative eyelid conditioning. As animals acquire the shock–tone association, DCN neurones begin to fire strongly immediately prior to shock onset. Furthermore, lesions, inactivation and local blockade of protein synthesis in the DCN can prevent acquisition of this task when applied before training and can eliminate the memory for training when applied afterwards (see Lavond (2002) for review). One cellular explanation for this memory trace has been that associative training ultimately produces long-term potentiation of those mossy fibre–DCN synapses that

 DOI: 10.1113/jphysiol.2004.071696

convey tone information (Medina *et al.* 2000). Another possible memory mechanism could involve changes in the intrinsic excitability of DCN neurones produced by training (see Hansel *et al.* (2001) for review). In this scheme, persistent changes in the properties of voltage-gated ion channels could result in altered firing rate or firing pattern as well as changes in the active, integrative properties of dendrites such as synaptic summation and spike backpropagation.

Indeed, there are now many examples, in both vertebrate and invertebrate model systems, of rapid, persistent changes in intrinsic neuronal excitability produced by behavioural training in intact animals or artificial synaptic stimulation in reduced preparations such as brain slices or cell cultures (see Zhang & Linden (2003) for review). In the DCN, prior work has shown that application of EPSP bursts to DCN neurones in a rat brain slice preparation gives rise to an increase in intrinsic excitability. Test pulses consisting of a fixed injection of depolarizing current evoke a greater number of spikes after a conditioning stimulus composed of EPSP bursts, and this increase persists for as long as the recordings can be maintained (>30 min). This phenomenon was blocked by application of an NMDA receptor antagonist and could be mimicked by repeated large injections of depolarizing current (Aizenman & Linden, 2000).

Here, we have combined microelectrode recording, whole-cell current-clamp recording and Ca^{2+} imaging to characterize intrinsic plasticity in the DCN of juvenile rat brain slices. We have sought to address the following questions. What electrophysiological sequelae accompany the induction in intrinsic excitability increases? Can increases in intrinsic excitability be manifested as changes in firing pattern? What is the range of stimuli that can induce increases in intrinsic excitability?

Methods

Slice preparation and microelectrode recording

Cerebellar slices were prepared as previously described (Aizenman *et al.* 1998). Briefly, juvenile (12- to 15-day-old) Sprague Dawley rats were killed by decapitation and the cerebellum was quickly removed and cooled with ice-cold standard artificial cerebrospinal fluid (ACSF). This procedure was approved by the Animal Care and Use Committee of The Johns Hopkins University School of Medicine. ACSF contained (mM): 124 NaCl, 5 KCl, 2.5 $CaCl_2$, 1.5 $MgSO_4$, 26 $NaHCO_3$, 1.25 NaH_2PO_4, and 20 D-glucose, and was equilibrated with 95% O_2–5% CO_2 to yield pH 7.4. Coronal slices of the cerebellum (400 μm thick) were cut on a vibrating tissue slicer (Leica VT1000S). After a 1 h recovery period at room temperature, slices were transferred to a Haas-style interface chamber. During recording, slices were continuously perfused at 32°C with standard ACSF at 2 ml min^{-1}. In some experiments, 200–300 μM picrotoxin or 2 mM kynurenic acid were added to the ACSF to block $GABA_A$ receptors and ionotropic glutamate receptors, respectively. Microelectrode intracellular recordings were made with borosilicate glass electrodes (100–150 MΩ) filled with 3 M K-acetate. A small hyperpolarizing bias current was applied to hold the membrane potential just below spike threshold. Synaptic tetani were applied via concentric bipolar stimulating electrodes placed in the white matter adjacent to the nuclei. Recordings were made from either the medial or lateral group of the DCN, and no differences were observed between the two nuclei. Excitatory synaptic stimuli (EPSP bursts), consisted of 10 bursts applied at 4 Hz; each burst comprising 10 pulses delivered at 100 Hz, repeated five times. EPSP bursts were delivered with 200–300 μM picrotoxin in the ACSF to block $GABA_A$-ergic transmission. Inhibitory synaptic stimuli (IPSP bursts) consisted of 20 bursts applied at 1 Hz, each burst comprising 10 pulses delivered at 100 Hz, applied with 2 mM kynurenic acid in the ACSF to block ionotropic glutamatergic transmission. This stimulation regime evoked a large number of rebound spikes. To record changes in intrinsic excitability, short depolarizing test pulses (300 ms, 0.05–0.3 nA) were applied. Recordings were made using an Axoclamp-2A amplifier (Axon Instruments). Recordings were filtered at 10 kHz, digitized at 10 kHz, and collected with a Macintosh computer running AxoGraph 4.6 software (Axon Instruments). Kynurenic acid was purchased from Tocris, UK. All other drugs were obtained from Sigma.

Data analysis

Data were analysed using AxoGraph 4.6 and Igor Pro software (WaveMetrics). The threshold for the first evoked spike (see Fig. 1*D*) was measured at the first point where the slope reached 20 V s^{-1}. The spike latency was measured from the onset of the test pulse to the peak of the first evoked spike. The slope of the depolarizing prepotential was calculated using a window 15–10 ms before the first evoked spike threshold. To measure the input resistance (R_{input}), a 100 ms-long, − 0.1 nA test pulse was delivered. R_{input} was calculated by curve fitting to the equation:

$$f(x) = V_{rest} - R_{input} \times \exp(-t/\tau).$$

To measure the changes in depolarizing sag and rebound depolarization-evoked action potentials, 300 ms long hyperpolarizing test pulses were used (Fig. 2). Depolarizing sag was measured from the voltage deflection peak to the steady-state plateau, the latter being determined by the mean value in a 10 ms window immediately prior to the end of test pulse(Fig. 2*A*). To measure the changes in the postburst potential (Fig. 3), four brief test pulses (2 ms, 2 nA) were applied at 5 ms

intervals, and the difference of the afterpotential following the four evoked spikes was measured in a window 10–20 ms after the end of the last test pulse. The response was measured three times with a 2 min interburst interval and the averages of the three traces before and 20 min after the conditioning stimulus (EPSP bursts) were compared.

In the analysis of bursting neurones (Fig. 4), the first interspike interval (ISI) was taken as the time between the first and the second evoked spike. The change in firing mode from burst to tonic was reflected as a decrease in the standard deviation (S.D.) of the normalized ISI. The ISI was normalized to its average. In *post hoc* comparisons of bursting neurones using input–output curves, the numbers of spikes evoked by different test pulses were normalized to those evoked by 0.1 nA. All values were expressed as mean ± S.E.M., and compared statistically

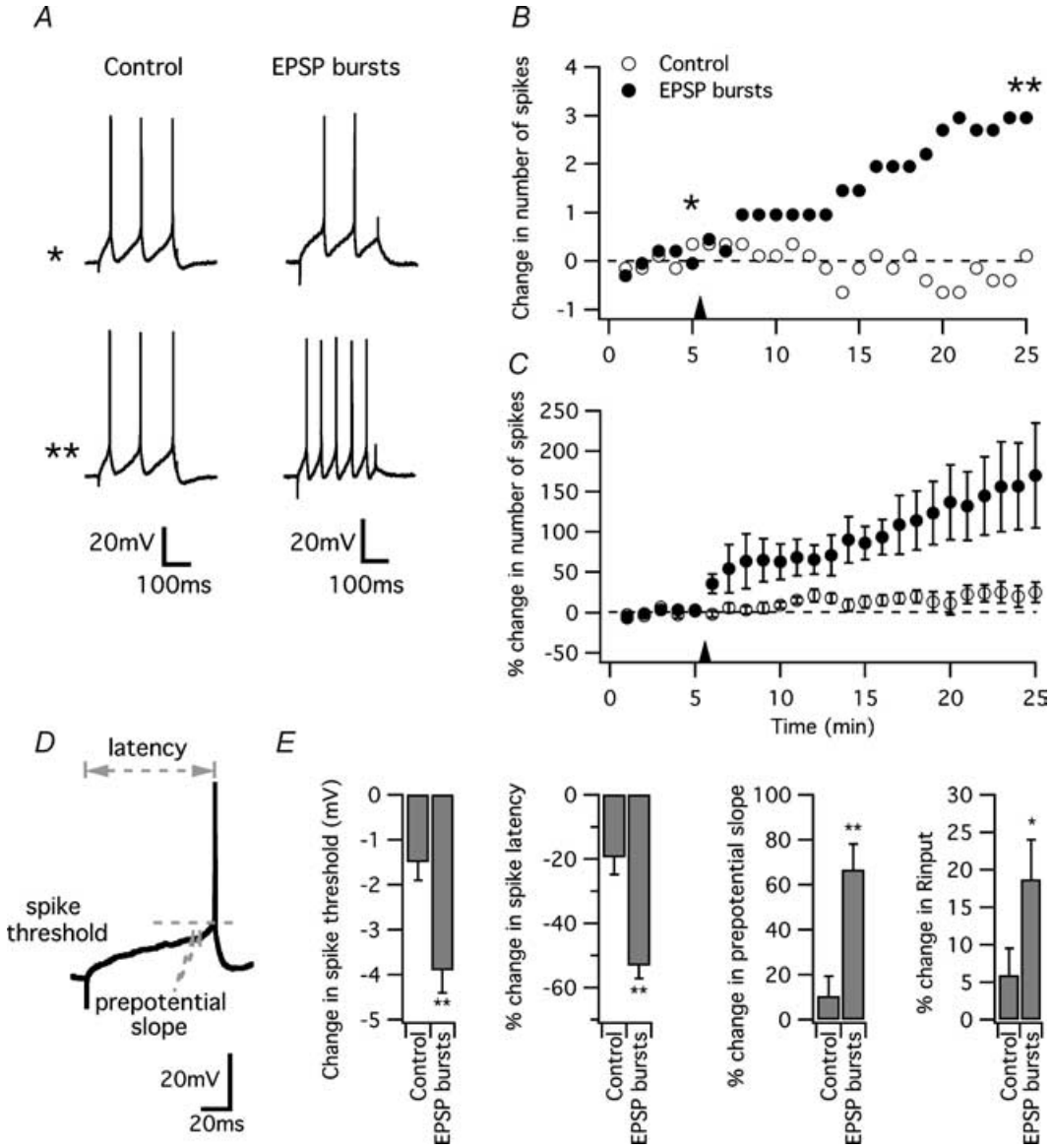

Figure 1. EPSP bursts induced a persistent increase in intrinsic excitability in deep cerebellar nuclear (DCN) neurones

A, sample traces showing action potentials evoked by a 300 ms test pulse in control and EPSP burst experiments. Traces are from time points indicated by asterisks on *B*. *B*, time course of changes in the number of spikes in representative control (○) and EPSP bursts (●) neurones. In EPSP burst experiments, following a 5 min baseline period, the neurone received excitatory synaptic stimuli consisting of 10 bursts applied at 4 Hz, each burst comprising 10 pulses delivered at 100 Hz, repeated five times (indicated by arrowhead). *C*, population means of percentage change in the number of spikes in control ($n = 9$) and EPSP bursts ($n = 11$) neurones. *D*, sample trace showing how various parameters of the first evoked spike were measured (as described in Methods). *E*, for each neurone, the mean value of each parameter was measured before ($t = 0$–5 min) and after ($t = 20$–25 min) the synaptic stimulation, and the percentage change was calculated.

using Mann–Whitney U-test. A significance of $P < 0.05$ was indicated by an asterisk, and a significance of $P < 0.01$ was indicated by two asterisks.

Whole-cell current-clamp recording and calcium imaging

Whole-cell patch recording was performed using 250-μm-thick coronal cerebellar slices. After a 1 h recovery period, slices were placed in a submerged chamber superfused with ACSF at 32°C. DCN neurones in the medial or lateral group were visualized through a 40 × water immersion objective using infrared Dodt gradient contrast optics (Luigs & Neumann, Ratingen, Germany), and whole-cell patch-clamp recordings were made with electrodes (3–6 MΩ) filled with internal saline containing (mM): 135 K-gluconate, 10 KCl, 10 Hepes, 4 Na_2-ATP, 0.4 Na-GTP, and 0.2 Oregon Green BAPTA-1, pH 7.2, osmolarity 290 for calcium imaging. To measure neuronal excitability after EPSP bursts, electrodes

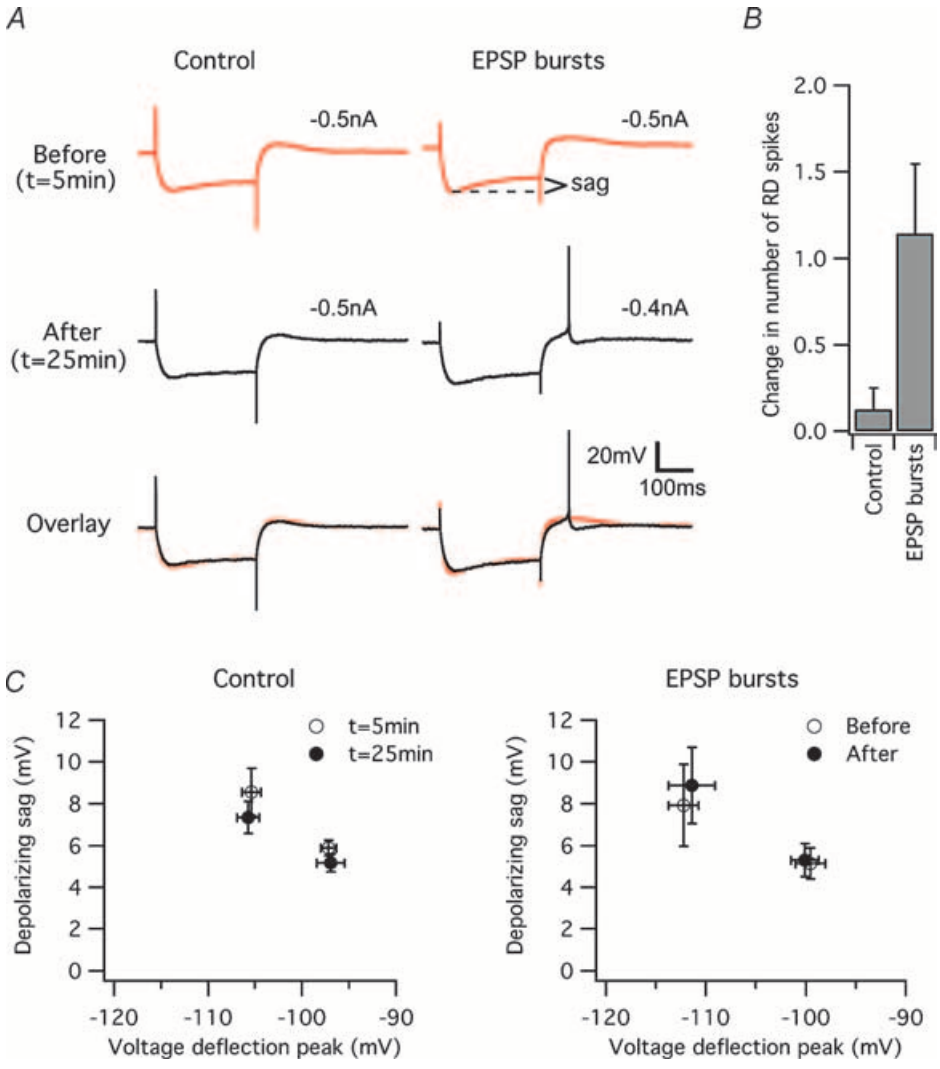

Figure 2. I_h channel modulation does not underlie the persistent increase in intrinsic excitability induced by EPSP bursts

A, sample traces of depolarizing sag, an index of I_h amplitude, induced by a −0.5 nA hyperpolarizing test pulse, obtained before ($t = 5$ min) and after ($t = 25$ min) the EPSP burst stimulation. In EPSP burst neurones the hyperpolarizing test pulse was reduced to −0.4 nA after conditioning stimulation to compensate for an increase in R_{input} and thereby match the hyperpolarizing voltage peak to the value obtained before stimulation. No obvious change in the depolarizing sag was observed, but a small increase in the number of rebound depolarization (RD) spikes was seen. *B*, the change in the number of RD spikes was compared between control ($n = 4$) and EPSP bursts ($n = 5$) neurones. *C*, the voltage deflection peak evoked by −0.3 nA and −0.5 nA hyperpolarizing test pulses, plotted against the depolarizing sag for a population of cells. In the EPSP burst plot, the hyperpolarizing test pulse was reduced after conditioning stimulation (EPSP bursts) so as to match the baseline voltage deflection peak to that before the stimulation. When the responses with matched voltage deflection peaks were compared, no change in the depolarizing sag was found.

were filled with internal saline containing (mM): 135 KCH_3SO_3, 5 KCl, 10 Hepes, 0.2 EGTA, 4 Na_2-ATP, 2 $MgCl_2$, 0.4 Na_3-GTP for control neurones, and filled with internal saline containing (mM): 111 KCH_3SO_3, 3 KCl, 10 Hepes, 12 BAPTA-K_4, 1 $MgCl_2$, 2 $CaCl_2$, 4 Na_2-ATP, 0.4 Na_3-GTP for BAPTA neurones. The ACSF was supplemented with 1 μM strychnine and 300 μM picrotoxin. To measure neuronal excitability after IPSP bursts, electrodes were filled with internal saline containing (mM): 125 KCH_3SO_3, 5 KCl, 10 Hepes, 4 Na_2-ATP, 0.4 Na_3-GTP, 2 $MgCl_2$, 0.2 EGTA, 10 phosphocreatine (di-tris salt) for control neurones, and filled with internal saline containing (mM): 98 KCH_3SO_3, 3 KCl, 10 Hepes, 4 Na_2-ATP, 0.4 Na_3-GTP, 1 $MgCl_2$, 12 BAPTA-K_4, 2 $CaCl_2$, 10 phosphocreatine (di-tris salt) for BAPTA neurones. The ACSF was supplemented with 3 mM kynurenic acid. Series resistance was <25 MΩ and was compensated at 70–80%. Synaptic burst stimulation was applied via a monopolar patch electrode filled with ACSF and placed in the white matter adjacent to the nuclei. Recordings were performed in current-clamp mode with either an Axopatch-1C or Axopatch 200B amplifier (Axon Instruments). Recordings of membrane voltage were filtered at 5 kHz, digitized at 10 kHz and collected with pClamp 9 software (Axon instruments). The imaging experiments began at least 30 min after break-in to allow for dye diffusion. Ca^{2+} imaging was performed with a Zeiss LSM 510 confocal microscope, using the 488 nm line of an argon laser for excitation, and emitted green fluorescence was detected through a 505 nm long-pass filter. The dendrites of DCN neurones typically elaborate in a three-dimensional fashion making it difficult to capture distal dendrites, proximal dendrites and soma in a single focal plane. To allow for simultaneous measurement in these compartments the pinhole was set wide open to maximize depth of field. A 128 × 128 pixel frame (1.3–2.5 μm pixel^{-1}) was scanned at a rate of 5–10 Hz. Background correction was performed by subtracting the background fluorescence of a representative neighbouring region next to the soma, proximal dendrite, or distal dendrite. Ca^{2+} signal amplitudes were expressed as $(F_t - F_0)/F_0$. The average fluorescence intensity in the baseline period was taken as F_0. At the end of experiment, the pinhole was closed to yield an Airy value of 1, z-stack confocal images were acquired and the neurone's image was reconstructed. Images were collected with Zeiss LSM software and analysed with Zeiss LSM and Igor Pro software. Oregon Green BAPTA-1 was purchased from Molecular Probes.

Results

The neurones of the DCN are composed of three different populations. Glutamatergic neurones project to premotor centres and tend to have large cell bodies. GABAergic neurones, which have smaller cell bodies, can either ramify their axon locally within the DCN or project to the inferior olive (or possibly, both). Previous work from this laboratory using a very similar microelectrode recording configuration showed that >95% of the recordings

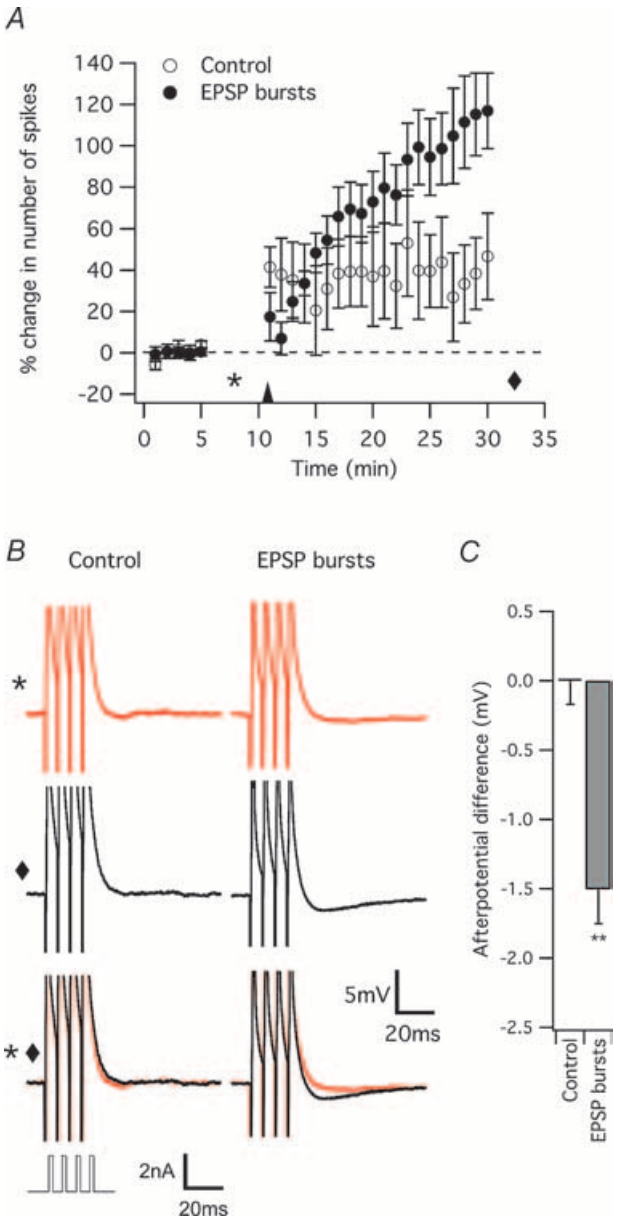

Figure 3. EPSP bursts induced a persistent hyperpolarizing shift in the post-spike-burst afterpotential
A, time course of the percentage change in the number of spikes evoked by 300 ms test pulses. After a 5 min baseline period, four compound 2 ms test pulses of 2 nA were given three times every 2 min to measure the afterpotential. The EPSP burst stimulation was delivered as indicated by the arrowhead. *B*, sample traces of afterpotentials evoked by four 2 ms compound test pulses, measured before (t = 5–10 min, indicated by asterisk in *A*) and after EPSP bursts (t = 30–35 min, indicated by diamond in *A*). Each trace is the average of three responses. *C*, mean changes in the afterpotential amplitude (n = 5/group).

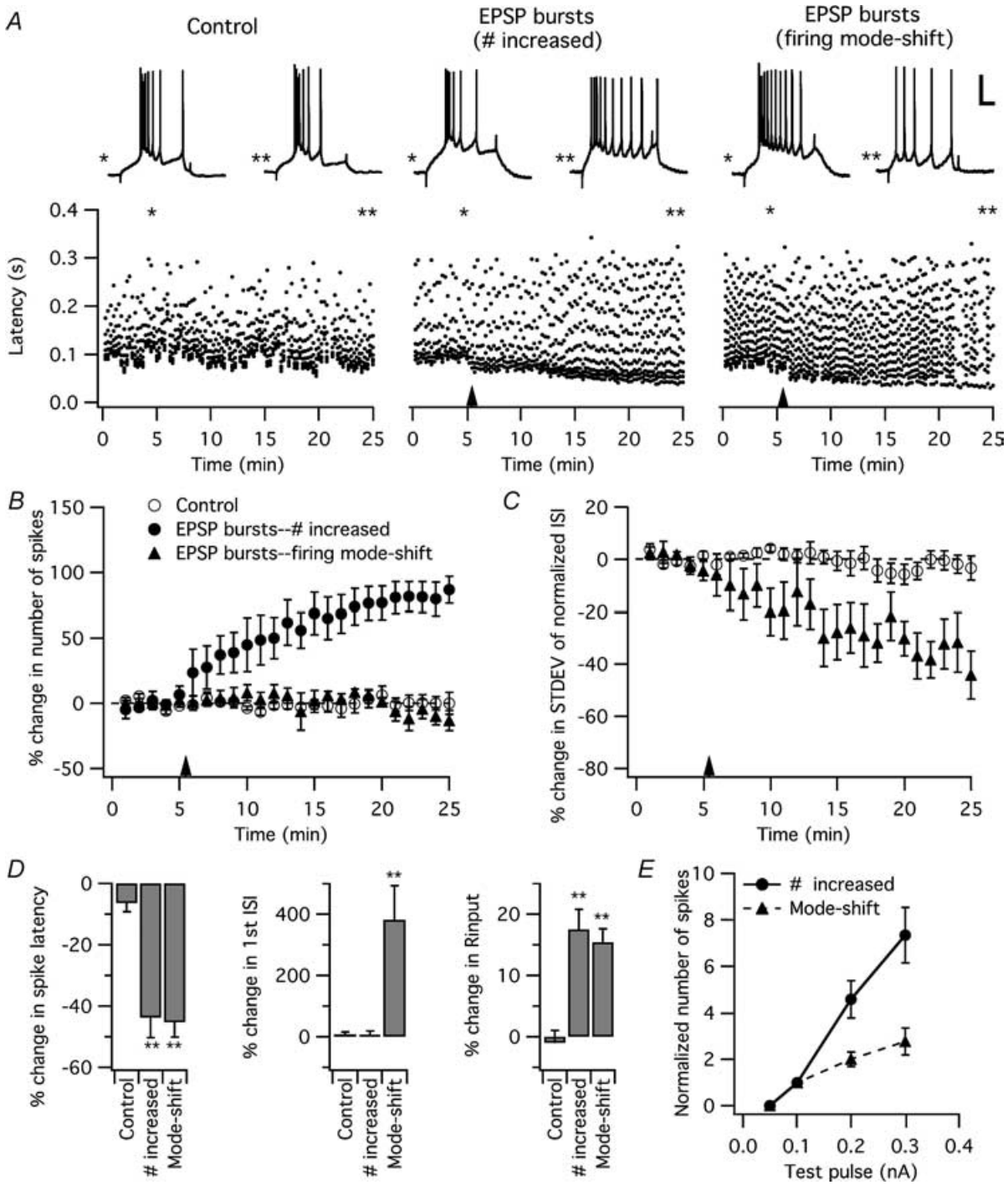

Figure 4. EPSP bursts induced either an increase in the number of depolarization-evoked spikes or a shift in firing mode in bursting DCN neurones

A, representative traces of responses of bursting neurones to a 300 ms depolarizing test pulse before (indicated by a single asterisk) and after (indicated by two asterisks) conditioning EPSP burst stimulation, and the corresponding time course plots of spike latency. Scale bars are 50 ms and 20 mV. EPSP burst stimulation is indicated by arrowheads. Neurones responded to EPSP bursts with either an increase in the number of spikes (middle panel shows a single representative cell), or a change in the firing mode (right panel). *B*, time course of the mean percentage change in the number of spikes evoked by test pulses ($n = 6$ cells/group). *C*, the percentage change in standard deviation of the interspike interval (ISI) in neurones which showed a firing mode change. The standard deviation of the ISI decreased after the stimulation, indicating a shift to a more tonic firing mode. *D*, percentage change in the first spike latency, the first interspike interval, and the R_{input}, measured before ($t = 0$–5 min) and after ($t = 20$–25 min) EPSP burst stimulation. *E*, the number of spikes evoked by depolarizing test pulses is plotted against

made with microelectrodes were from large, presumably glutamatergic, neurones (Aizenman *et al.* 2003). Within this population, there is also variability in spiking pattern. While there is a continuum of diverse spiking behaviour, in general, 44% of the neurones recorded in this study responded to depolarizing current injection with tonic firing (Fig. 1*A*) while 56% exhibited some form of bursting behaviour (Fig. 4*A*). Initially, we will discuss experiments performed with tonic firing DCN neurones.

Intrinsic excitability was measured by continually injecting a small hyperpolarizing bias current to silence ongoing spike firing, and then injecting a 300-ms-long depolarizing current (0.1–0.2 nA) sufficient to evoke a small number of spikes (typically 2–3; Fig. 1*A*). These experiments were performed in picrotoxin-containing external saline to block $GABA_A$ receptors. The depolarizing test pulse was delivered every 15 s and responses were fairly stable over a 25 min recording period (Figs 1*B* and *C*; mean change in number of spikes: 0.55 ± 0.25 spikes; $22 \pm 12\%$ change relative to baseline; $n = 9$). In a separate population of cells, after a 5-min period of baseline recording, a conditioning stimulus was given consisting of high-frequency burst stimuli delivered through a stimulating electrode placed in the adjacent white matter to evoke EPSPs. This resulted in a slow, sustained increase in the number of action potentials evoked by the depolarizing test pulse (Fig. 1*B* and *C*; 2.82 ± 0.45 spikes; $152 \pm 53\%$ change; measured at $t = 20$–25 min; $n = 11$, $P < 0.05$ compared to control group) as previously reported (Aizenman & Linden, 2000). A number of other measurements could also be derived from this experiment. EPSP bursts resulted in a significant reduction of spike threshold (Fig. 1*E*; measured for the first evoked spike; -3.9 ± 0.5 mV) and the latency to the first spike ($-53 \pm 4\%$ change). The slope of the depolarizing prepotential (which intervenes between current injection and the first spike threshold) was also significantly increased following EPSP bursts ($67 \pm 11\%$ change). R_{input}, monitored using a 100-ms-long, 0.1 nA hyperpolarizing test pulse, was also persistently increased by the conditioning stimulation, although this was a small effect ($19 \pm 5\%$ change). The increase in R_{input} is unlikely to underlie the persistent increase in the number of evoked spikes as these two measures were uncorrelated across the population of cells which received EPSP bursts ($r^2 = 0.067$, $P > 0.05$; Supplementary Fig. 1). Overall, the persistent effects of EPSP bursts may reflect an alteration of one or more types of voltage-gated ion channels, some of which operate at or below spike threshold.

One current which has an important role in regulating subthreshold excitability is the hyperpolarization-activated cation conductance, I_h. This current is subject to both short- and long-term modulation. Previous work has shown that induction of febrile seizures in young rats results in a persistent increase of I_h in hippocampal pyramidal neurones (Chen *et al.* 2001). Application of the anticonvulsant drug limotrigine also decreases dendritic excitability through an increase in dendritic I_h in hippocampal pyramidal neurones (Poolos *et al.* 2002). To test the hypothesis that persistent increases in intrinsic excitability in the DCN are associated with alterations in I_h, we used 300-ms-long injections of negative current as test pulses (-0.3 to -0.5 nA). These test pulses evoked an initial hyperpolarization that was then attenuated by the development of a depolarizing 'sag' in the voltage response, typically attributed to I_h. The amplitude of this depolarizing sag is greater with larger injections of negative current (Jafri & Weinreich, 1998; Aizenman & Linden, 1999; Chen *et al.* 2001; Williams *et al.* 2002). Following the termination of the test pulse there is a rebound depolarization, the size of which is also proportional to the peak amplitude of the hyperpolarization (Aizenman & Linden, 1999). If sufficiently large, this rebound depolarization can evoke one or more Na^+ spikes. Following, EPSP bursts, the injection of a constant test pulse gave rise to a larger peak hyperpolarization, which can be attributed to the previously measured increase in R_{input} (Fig. 1*E*). Consistent with previous reports (Jafri & Weinreich, 1998), this caused a greater degree of sag as a consequence of the larger peak hyperpolarization. However, when the amplitude of the negative current test pulse was reduced to match the baseline peak hyperpolarization, the amplitude of the depolarizing sag was unchanged (Fig. 2*A* and *C*; 5.1 ± 0.8 mV before EPSP bursts, 5.3 ± 0.8 mV after EPSP bursts, $n = 5$). Therefore, modulation of I_h is unlikely to underlie persistent increases in intrinsic excitability produced by EPSP bursts. Interestingly, the probability of evoking an action potential during the subsequent rebound depolarization was increased, even when the test pulses were reduced after EPSP bursts to match the baseline peak hyperpolarization (Fig. 2*A* and *B*; $P = 0.055$).

Bursts of Na^+ spikes are often followed by an afterpotential, either an afterhyperpolarization (AHP) or an afterdepolarization (ADP). Several conductances can contribute to these afterpotentials including the Ca^{2+}- and voltage-sensitive current, I_C, voltage-sensitive

the magnitude of the injected current, normalized to the number of spikes evoked by a 0.1 nA test pulse. The measurement was taken before the synaptic tetanus and *post hoc* analysis was subsequently performed. Bursting neurones which showed an increase in the number of spikes after stimulation ($n = 4$) were more excitable than bursting neurones which showed a firing mode change ($n = 4$).

Ca^{2+} currents, the Ca^{2+}-sensitive K^+-current, mI_{AHP}, the voltage-sensitive K^+-current, I_M, and the Ca^{2+}-sensitive K^+-current, sI_{AHP} (see Storm (1990) for review). To determine whether these afterpotentials are persistently altered following EPSP bursts we used a hybrid stimulation protocol. First, responses to the standard 300-ms-long depolarizing test pulse were recorded for 5 min and then we switched to a compound test pulse consisting of four 2-ms-long large positive current injections (2 nA) delivered every 7 ms repeated every 60 s. This compound test pulse evoked a set of four Na^+ spikes with consistent timing, followed by an afterpotential. After delivery of the EPSP burst conditioning stimulus, simple depolarizing step test pulses were resumed for

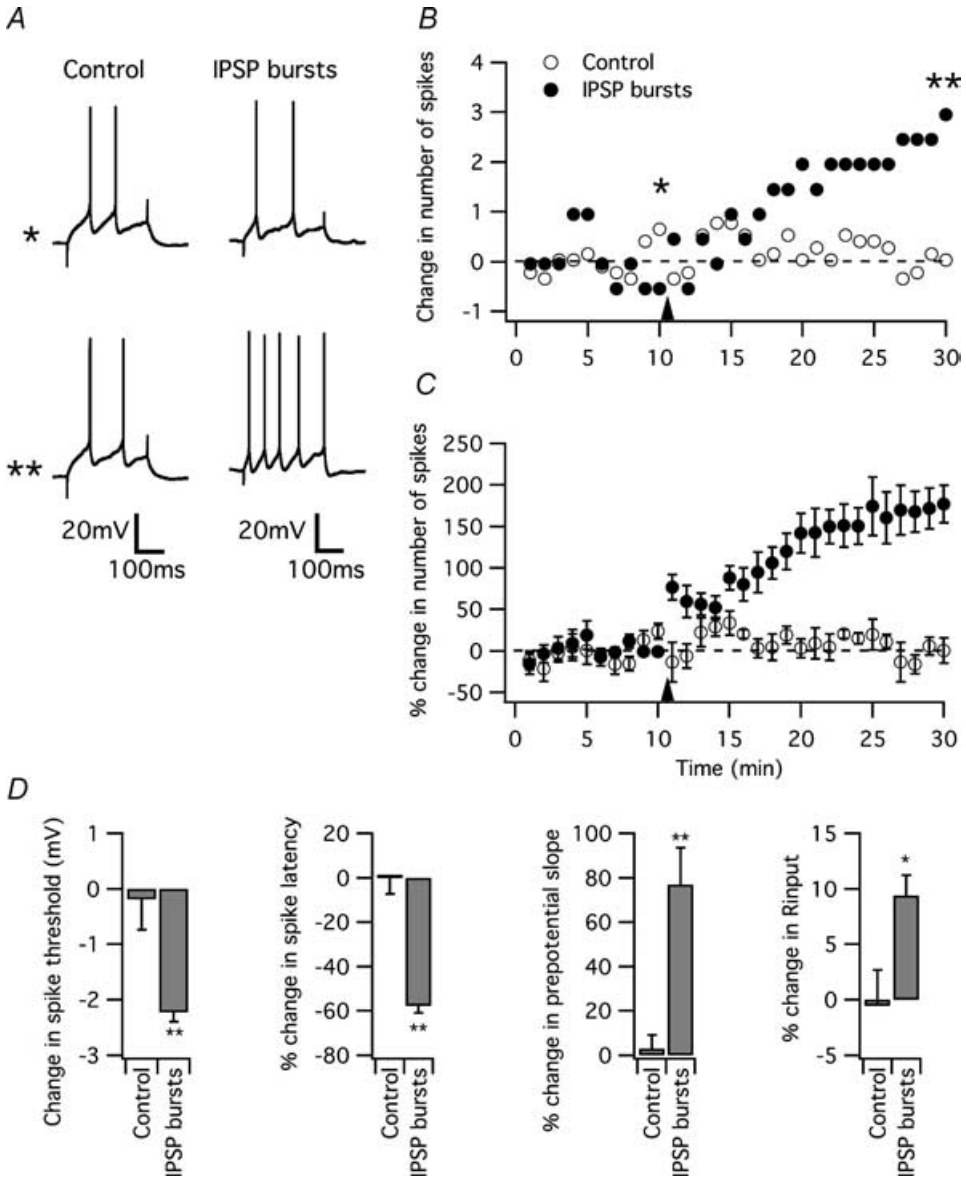

Figure 5. IPSP bursts induced a persistent increase in intrinsic excitability in DCN neurones
A, representative traces showing action potentials evoked by a 300 ms test pulse in control and IPSP burst experiments. Traces are from time points indicated by asterisks in *B*. *B*, time course of changes in the number of spikes in representative control (○) and IPSP bursts (●) neurones. In IPSP burst experiments, following a 10 min baseline period, the neurone received inhibitory synaptic conditioning stimuli consisting of 20 bursts applied at 1 Hz, each burst comprising 10 pulses delivered at 100 Hz (indicated by arrowhead). *C*, averaged time course of percentage change in the number of spikes in control ($n = 4$) and IPSP burst ($n = 6$) neurones. *D*, for each neurone, the average value of each parameter was measured before ($t = 5$–10 min) and after ($t = 25$–30 min) the synaptic stimulation, and the percentage change was calculated and compared between the control and IPSP burst groups.

20 min, followed by another set of compound test pulses (Fig. 3). The main finding of this experiment was that EPSP bursts produced a significant shift in the afterpotential in the hyperpolarizing direction (Fig. 3*B* and *C*; -1.5 ± 0.2 mV, $n = 5$), sometimes resulting in the conversion of an ADP to an AHP. This increase in the rate and extent of repolarization may help to speed Na^+ channel de-inactivation thereby supporting an increase in spike frequency.

Consistent with previous findings (Aizenman & Linden, 2000; Fig. 1), the standard 300-ms-long test pulses revealed a significant increase in the number of evoked spikes following EPSP bursts (Fig. 3*A*; 2.8 ± 0.3 spikes, $109 \pm 20\%$ increase, $n = 5$). However, the control group also showed a small increase in excitability (0.6 ± 0.2 spikes, $38 \pm 20\%$ increase, $n = 5$), probably because the compound test pulses themselves were sufficient to evoke a small degree of intrinsic plasticity. Despite the small increase in excitability of the control group, neurones in the EPSP burst group still showed a significant increase in the number of evoked spikes when compared to control ($P < 0.05$).

To this point, we have only considered intrinsic plasticity in tonic firing DCN neurones. Bursting neurones show a range of firing patterns in response to a 300 ms depolarizing step. Some show a simple burst-and relax-pattern (Fig. 4*A*), while others may fire one or two spikes at lower frequency before burst onset. The duration of the burst can also vary considerably from neurone to neurone. However, for a single neurone, the pattern of spiking in response to a depolarizing test pulse is reasonably stable (Fig. 4*A*). Following EPSP bursts, intrinsically burst-firing cells showed one of two forms of modulation: 6 of 12 cells showed a persistent increase in the number of depolarization-evoked spikes similar to that seen in tonic firing cells (Fig. 4*B*; $82 \pm 11\%$ change, $P < 0.01$ compared to control group). The other six cells showed no significant change in the number of spikes ($-9 \pm 6\%$ change, $P = 0.31$ compared to control group), but rather a shift in the firing mode from bursting to tonic firing. This was reflected in a significant increase of the first interspike interval in the cells which showed a firing mode shift (Fig. 4*D*; $381 \pm 111\%$ change) but not in those in which the number of evoked spikes was increased ($6 \pm 13\%$ change), nor in control cells ($8 \pm 8\%$ change, $n = 7$). To further quantify the firing mode, interspike intervals were calculated and normalized to their mean value. The S.D. of the normalized interspike intervals was then calculated. In the control group, this value was quite stable over the recording period (Fig. 4*C*; $-2 \pm 3\%$ change). However, in the cells which received EPSP bursts and showed a mode-shift, the percentage change in the S.D. of the normalized interspike interval decreased ($-32 \pm 9\%$ change, $P < 0.01$ compared to control group), indicating a shift to a more tonic firing pattern.

What accounts for the difference between the bursting cells which show an increase in the number of evoked spikes *versus* those that show no increase but shift firing mode? These two groups showed similar reductions in the latency of the first evoked spike and a similar small increase in R_{input}. One difference emerged when examining a baseline input/output function for depolarizing current injection. *Post hoc* analysis showed that those cells which responded to EPSP bursts with a firing mode-shift were less excitable in the baseline state: they produced fewer spikes in response to increasing 300-ms-long injections of depolarizing current (Fig. 4*E*).

DCN neurones show rebound depolarization after stimulation by IPSP bursts. Indeed, previous work has shown that IPSP bursts can trigger LTP and LTD of the Purkinje cell–DCN synapse (Aizenman *et al.* 1998). We investigated whether IPSP bursts could similarly trigger changes in intrinsic excitability in tonic firing DCN neurones. IPSP bursts (each consisting of 10 pulses at 100 Hz, repeated with a burst frequency of 1 Hz for 20 repetitions) caused DCN neurones to respond to depolarizing test pulses with a larger number of spikes (Fig. 5*A–C*; 3.2 ± 0.3 spikes, $169 \pm 26\%$ change, $n = 6$, $P < 0.01$ compared to control group). As seen previously with EPSP bursts, this was associated with a reduction in spike threshold (Fig. 5*D*; -2.2 ± 0.2 mV) and first spike latency ($-58 \pm 3\%$ change) as well an increase in the slope of the depolarizing prepotential ($77 \pm 17\%$ change) and R_{input}. ($9 \pm 2\%$ change). The increase in R_{input} is unlikely to underlie the persistent increase in the number of evoked spikes as these two measures were uncorrelated across the population of cells which received IPSP bursts ($r^2 = 0.0003$, $P > 0.05$; Supplementary Fig. 1). Hence, at least in tonic firing DCN neurones, IPSP and EPSP bursts can produce similar persistent increases in intrinsic excitability.

Previous work has shown that increases in intrinsic excitability of DCN neurones produced by EPSP bursts could be blocked by an NMDA receptor antagonist. Furthermore, a similar, albeit weaker, increase in intrinsic excitability could be produced by repeated large injections of depolarizing current (intracellular tetani) and this was eliminated with application of Cd^{2+} ions, a nonspecific blocker of Ca^{2+} channels (Aizenman & Linden, 2000). Together, these results suggest that Ca^{2+} transients are required for intrinsic plasticity in the DCN. Previous work has also shown that Ca^{2+} transients in the soma and proximal dendrite of DCN cells may be driven by sustained depolarization sufficient to evoke spike firing (Muri & Knopfel, 1994), a depolarizing step delivered in voltage-clamp mode (Gauck *et al.* 2001) or the rebound spiking which follows a hyperpolarizing current injection (Aizenman *et al.* 1998). Here, we have sought to measure the Ca^{2+} transients in DCN neurones produced by EPSP and IPSP burst stimulation in distal dendrites, where many

excitatory synapses are received (Chan-Palay, 1977), as well as in the proximal dendrites and soma.

Whole-cell current-clamp recording was used to measure membrane voltage and to deliver the Ca^{2+} reporter dye Oregon Green BAPTA-1, which was excited by an argon ion laser on a scanning confocal microscope. Following a period of ~30 min for dye equilibration, measurements were made using the microscope with the pinhole wide open in order to maximize depth of field and follow the course of a dendrite through the z-dimension, and thereby allow for simultaneous measurement of multiple regions (Fig. 6*B*). The proximal dendrite was defined as that within 50 μm (three-dimensional distance) of the soma while the distal dendrite was at least 100 μm (three-dimensional distance) from the soma. EPSP bursts (identical to those used previously for intrinsic plasticity experiments) produced bursts of spikes. A set of 10 bursts of 10 EPSPs each produced a Ca^{2+} transient which was largest in the distal dendrite (Fig. 6*A*; $\Delta F/F = 0.68$ for the peak transient of the first set) and which was diminished in the proximal dendrite ($\Delta F/F = 0.31$) and further reduced in the soma ($\Delta F/F = 0.07$). This pattern was also reflected in the population of cells measured in this fashion: the first peak amplitude of the Ca^{2+} response in the proximal dendrite was 45% ± 6% of that in the distal dendrite ($n = 4$).

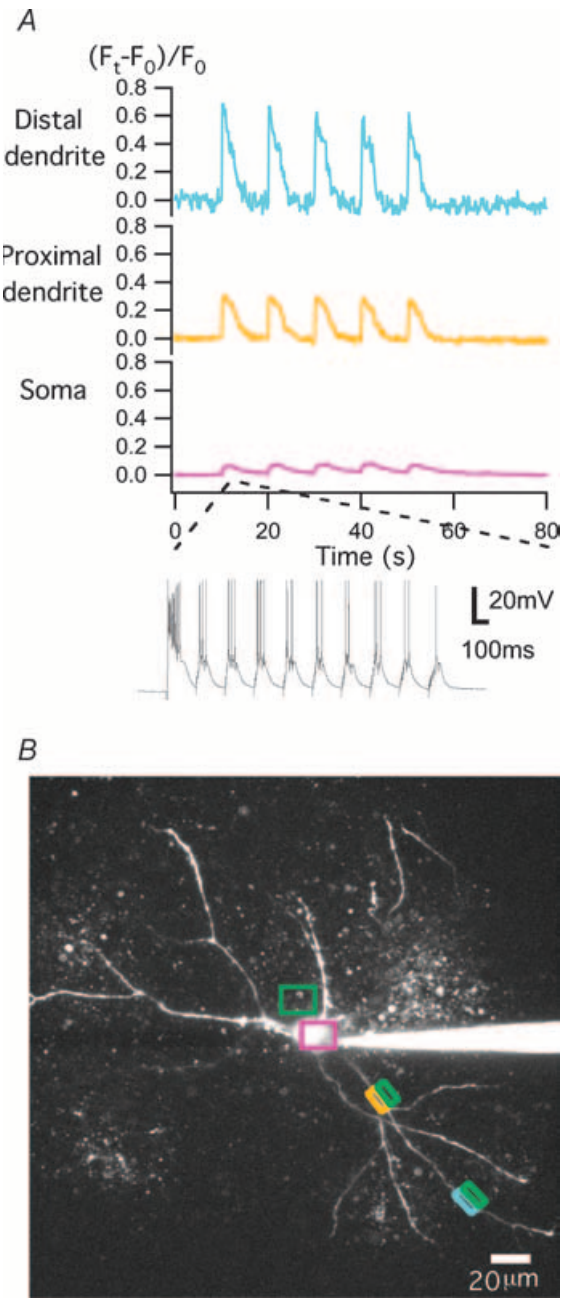

Figure 6. Ca^{2+} transients evoked by EPSP bursts in DCN neurones
A, normalized increases in background-subtracted fluorescence intensity due to Ca^{2+} transients evoked by EPSP burst stimuli are recorded simultaneously in the soma, and the proximal and distal dendrite in a representative neurone. Membrane voltage responses evoked by EPSP bursts are shown as an inset. *B*, confocal image of a DCN neurone showing the somatic, and proximal and distal dendritic regions that were examined for analysis of Ca^{2+} transients. Corresponding background regions are indicated with green boxes.

IPSP bursts are an effective means of driving rebound spiking in DCN cells (Aizenman & Linden, 1999), so it is reasonable to suspect that they might also effectively drive Ca^{2+} transients. Ca^{2+} imaging was performed together with delivery of IPSP bursts (identical to those used previously for intrinsic plasticity experiments). In these cells (as with some of those used with EPSP bursts), setting the detector gain to resolve the distal dendrite resulted in saturation of the somatic signal, so the imaging was done in two separate runs: once with high detector gain to measure the distal and proximal dendrite simultaneously and once with low detector gain to measure the proximal dendrite and soma (Fig. 7*A* and *B*). While the spiking measured during these two different runs was quite similar, there are small trial-to-trial variations in the number of spikes and their timing which cause a small degree of variability in the amplitude and kinetics of Ca^{2+} transients. IPSP bursts (and their subsequent rebound spiking) produced Ca^{2+} transients that were roughly similar to those evoked by EPSP bursts. They were greatest in the distal dendrite (Fig. 7*B*; $\Delta F/F = 0.49$ at high gain) and decreased in the proximal dendrite ($\Delta F/F = 0.21$ at high gain, 0.31 at low gain) and further decreased in the soma ($\Delta F/F = 0.12$ at low gain). The first peak amplitude of the Ca^{2+} response in the proximal dendrite was 54% ± 11% of that in the distal dendrite ($n = 3$). The distal dendritic response showed individual peaks evoked by each burst superimposed upon a plateau, whereas the individual burst responses in the proximal dendrite and soma decayed so slowly as to fuse. Thus, both EPSP and IPSP bursts can drive Ca^{2+} responses which are larger in amplitude in the distal dendrites compared to the proximal dendrites and soma.

While previous work has shown that an NMDA receptor antagonist can block excitability increases induced by EPSP bursts, and a broad-spectrum Ca^{2+} channel blocker (external $CdCl_2$) can block excitability increases induced by intracellular tetani (Aizenman *et al.* 2000), there is no direct evidence to show that postsynaptic Ca^{2+} transients are necessary for inducing increases in intrinsic excitability. We used whole-cell current clamping to internally perfuse the calcium chelator BAPTA, and measured the neuronal response to 300 ms depolarizing test pulses before and after application of EPSP bursts (identical to those in previous experiments). All neurones obtained were burst firing when BAPTA was present in the internal saline, a phenomenon which has been previously observed with microelectrode recordings (Aizenman & Linden, 1999). In control neurones, EPSP bursts caused a persistent increase in the number of spikes evoked by a depolarizing current injection test pulse (Fig. 8*A–C*; $50 \pm 5\%$ change, $n = 5$), decreases in spike threshold (Fig. 8*D*; -0.9 ± 0.2 mV) and latency ($-26 \pm 5\%$ change), and increases in prepotential

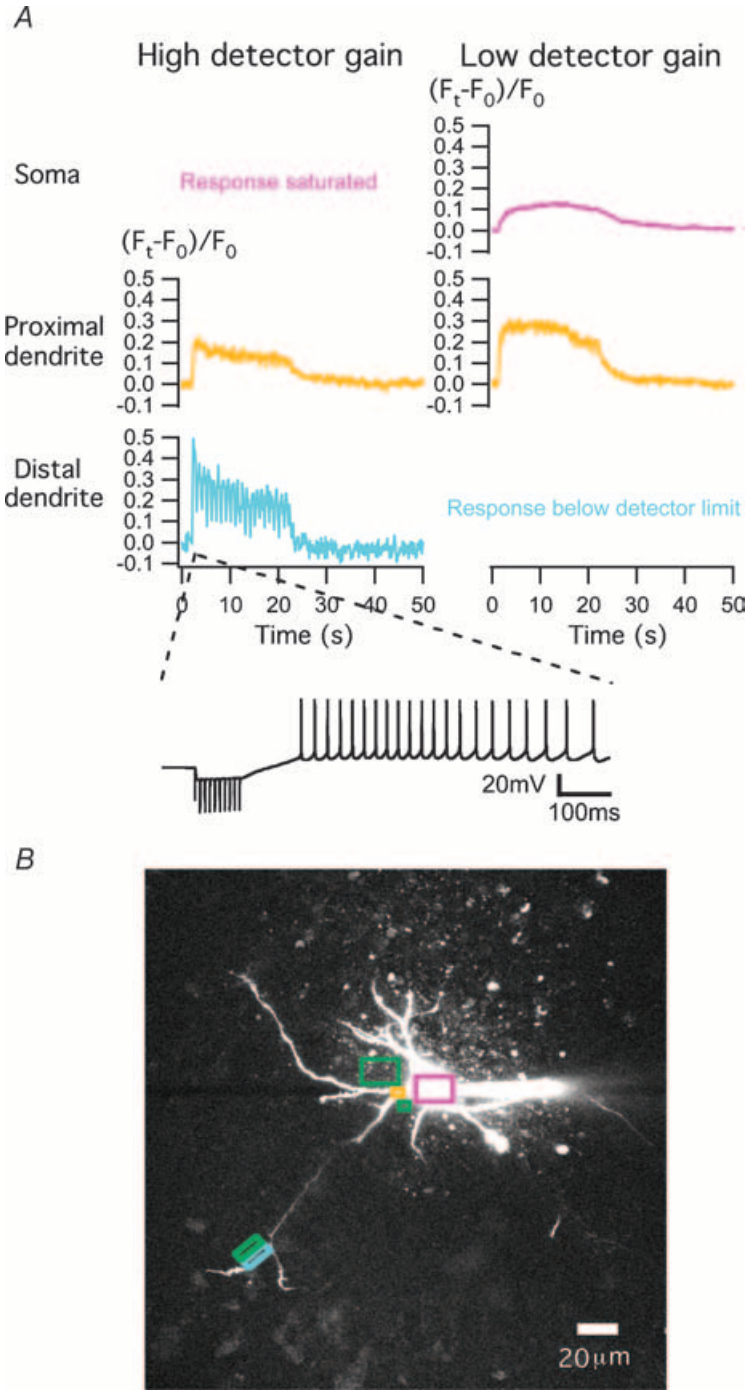

Figure 7. Ca^{2+} transients evoked by IPSP bursts in DCN neurones
A, normalized increases in background-subtracted fluorescence intensity due to Ca^{2+} transients evoked by IPSP burst stimuli. The high detector gain used to obtain an adequate distal dendrite signal gave a saturated signal in the soma (left panels), while the low detector gain used to resolve the somatic signal gave yielded responses in the distal dendrites that were too small to reliably measure (right panels), so measurements were made in two separate passes. The IPSP burst and subsequent rebound spikes are shown in the inset. *B*, confocal image of a DCN neurone showing analysis boxes. The background regions used for background-subtracted measures are indicated with green boxes.

slope ($14 \pm 12\%$ change) and R_{input} ($13 \pm 2\%$ change). The pattern of changes seen here was similar to the responses of neurones in the microelectrode recording configuration, but the changes were somewhat smaller in amplitude (compare with Fig. 1). In neurones perfused with BAPTA, EPSP bursts caused a transient decrease in the number of evoked spikes, which recovered to baseline within 15 min. Neurones perfused with BAPTA did not show a persistent change in the number of evoked spikes (Fig. 8*A*–*C*; $2 \pm 7\%$ change, $n = 6$, $P < 0.01$ compared to control), nor did they show any significant changes in spike threshold (Fig. 8*D*; -0.4 ± 0.1 mV), latency ($-1 \pm 3\%$ change), prepotential slope ($-1 \pm 1\%$ change) and R_{input} ($-3 \pm 2\%$ change). There are two lines

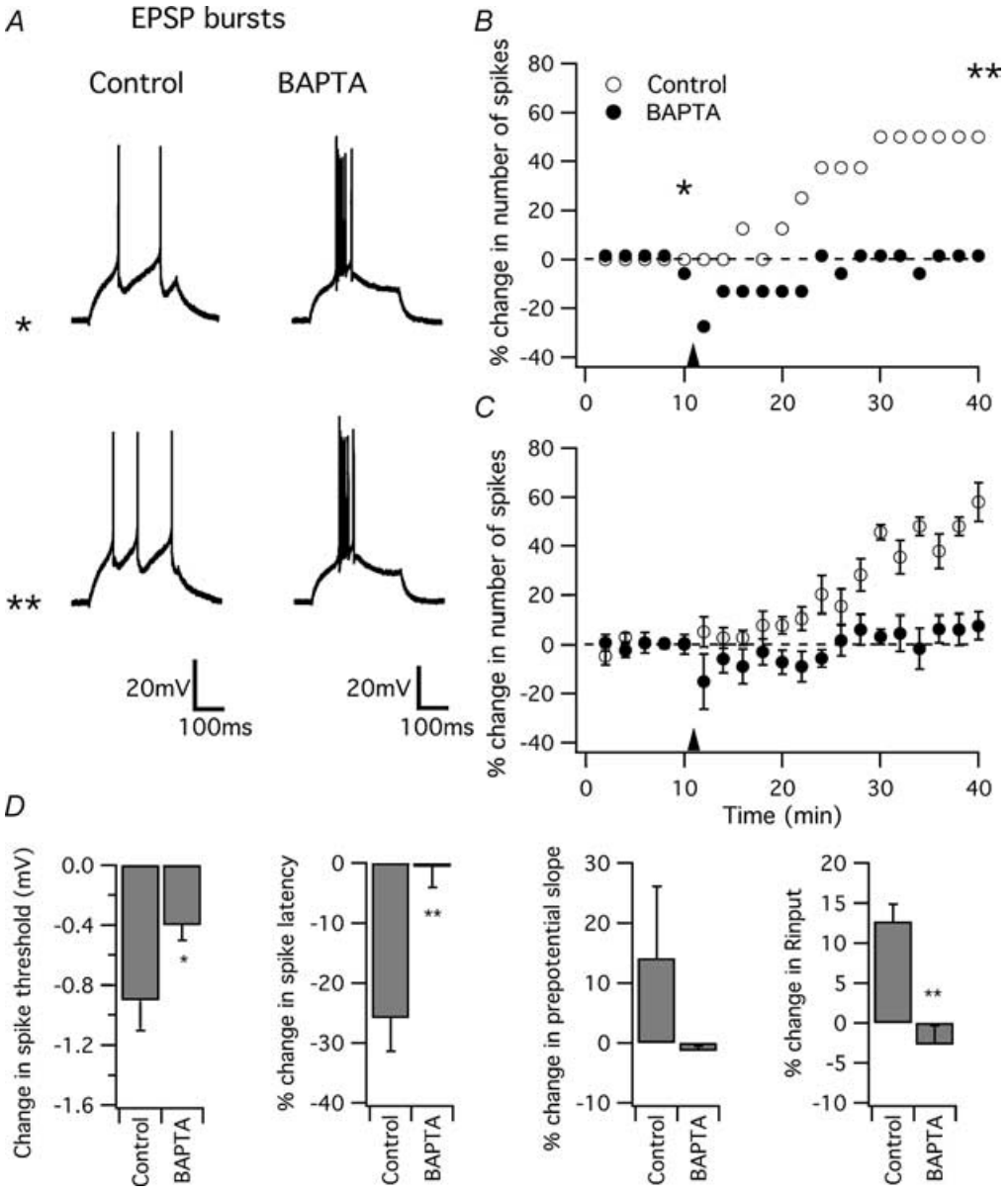

Figure 8. Postsynaptic Ca^{2+} transients are necessary for the induction of an excitability increase by EPSP bursts

A, representative traces showing action potentials evoked by a 300 ms test pulse in control and BAPTA experiments, before and after EPSP bursts stimulation. Traces are from time points indicated by asterisks in *B*. *B*, time course of percentage change in the number of spikes in representative control (○) and BAPTA (●) neurones. In both groups, following a 10 min baseline period, an EPSP bursts stimulus was applied, consisting of 10 bursts applied at 4 Hz, each burst comprising 10 pulses delivered at 100 Hz, repeated five times (indicated by arrowhead). *C*, averaged time course of percentage change in the number of spikes in control ($n = 5$) and BAPTA ($n = 6$) neurones. *D*, for each neurone, the average value of each parameter was measured before ($t = 0$–10 min) and after ($t = 20$–30 min) the synaptic stimulation, and the percentage change was calculated and compared between the control and BAPTA groups.

of evidence to suggest that BAPTA application did not block increases in intrinsic excitability by driving the neurones to their maximal firing rate and thereby causing response saturation. First, the use of a smaller test pulse before and after EPSP bursts did not reveal an increase in excitability in BAPTA (Supplementary Fig. 2*A*). Second, after the EPSP bursts recorded in BAPTA, a larger test pulse than the one used in Fig. 8 elicited a greater number of spikes, indicating that the neuronal response was submaximal (Supplementary Fig. 2*B*).

Similar experiments were performed to investigate whether BAPTA can block the increase in intrinsic excitability induced by IPSP bursts. In control neurones, IPSP bursts caused a persistent increase in the number of spikes evoked by the depolarizing test pulse (Fig. 9*A*–*C*; $53 \pm 3\%$ change, $n = 5$), as well as decreases in spike

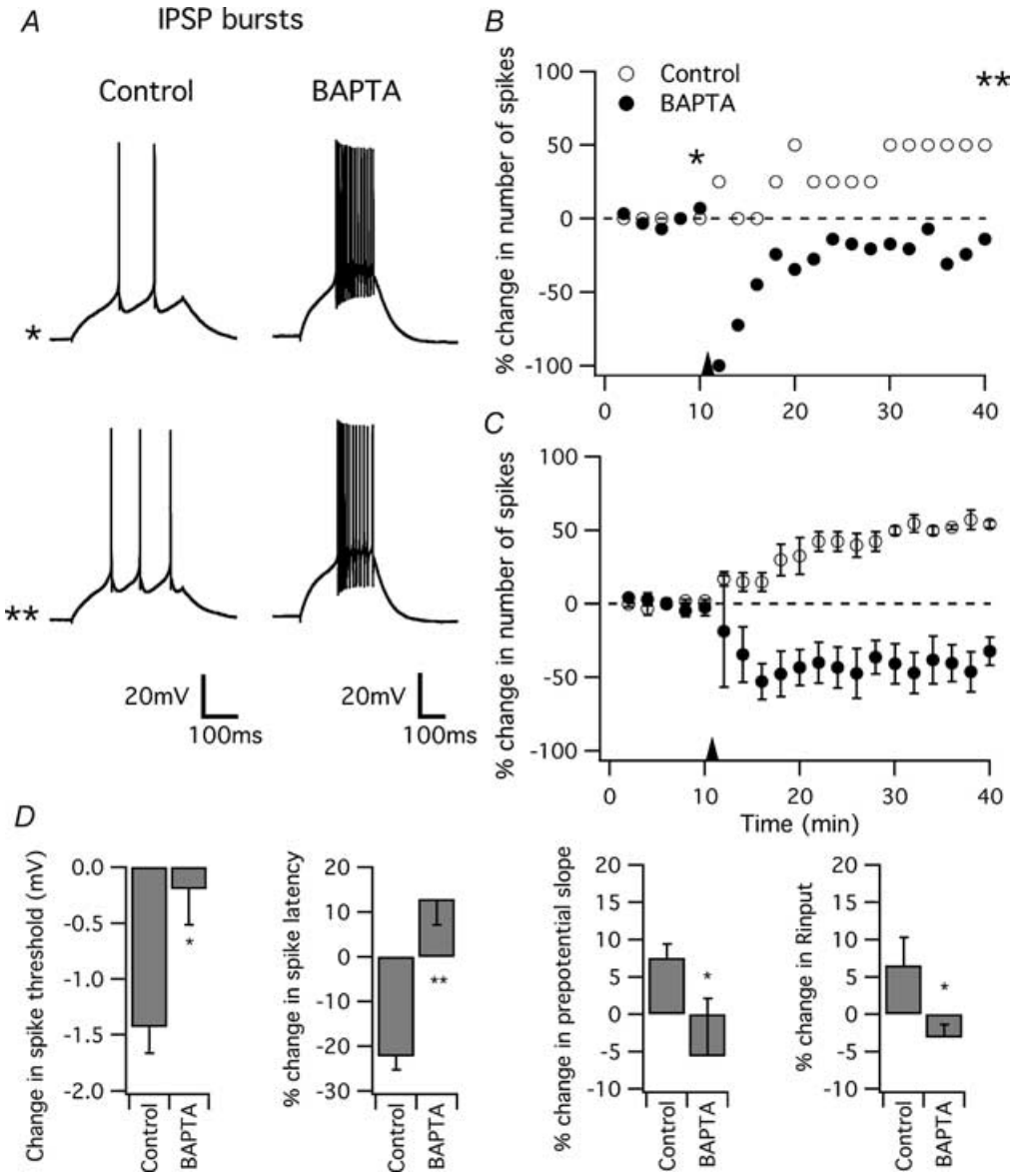

Figure 9. Postsynaptic Ca^{2+} transients are necessary for the induction of an excitability increase by IPSP bursts

A, Representative traces showing action potentials evoked by a 300 ms test pulse in control and BAPTA experiments, before and after IPSP bursts stimulation. Traces are from time points indicated by asterisks in *B*. *B*, time course of percentage change in the number of spikes in representative control (○) and BAPTA (●) neurones. In both groups, following a 10 min baseline period, an IPSP bursts stimulus was applied, consisting of 20 bursts applied at 1 Hz, each burst comprising 10 pulses delivered at 100 Hz (indicated by arrowhead). *C*, averaged time course of percentage change in the number of spikes in control ($n = 5$) and BAPTA ($n = 6$) neurones. *D*, for each neurone, the average value of each parameter was measured before ($t = 0$–10 min) and after ($t = 20$–30 min) the synaptic stimulation, and the percentage change was calculated and compared between the control and BAPTA groups.

threshold (Fig. 9*D*; -1.4 ± 0.2 mV) and first spike latency (-22 ± 3% change), and increases in prepotential slope (8 ± 2% change) and R_{input} (7 ± 4% change). In neurones internally perfused with BAPTA, IPSP bursts caused a transient large change in the number of spikes evoked, which recovered to a plateau at -41 ± 13% of the baseline level (Fig. 9*A–C*; $n = 6$). This persistent decrease in the number of spikes evoked in BAPTA neurones may be due to an increase in tonic inhibition. BAPTA also blocks changes in spike threshold (Fig. 9*D*; -0.2 ± 0.3 mV), prepoptential slope (-6 ± 8% change) and R_{input} (-3 ± 2% change), and caused an increase in first spike latency (13 ± 6% change). Hence, this experiment formally shows that postsynaptic Ca^{2+} transients are necessary for induction of intrinsic excitability increases.

Discussion

There are several main findings in the present report. EPSP bursts produce a persistent change in the intrinsic properties of DCN neurones. In tonic firing DCN neurones this is manifested as an increase in the number of spikes evoked by either a depolarizing step (Fig. 1) or the rebound depolarization following a hyperpolarizing step (Fig. 2). This increase in excitability is accompanied by a reduction in spike threshold and latency and increases in R_{input} and the prepotential slope. It is also accompanied by a hyperpolarizing shift in the afterpotential following an evoked spike burst (Fig. 3), but not in the hyperpolarization-evoked 'depolarizing sag', an index of I_h (Fig. 2). Similar changes in neuronal intrinsic excitability have been reported in both invertebrate and vertebrate preparations (see Zhang & Linden, 2003, for review). In the cerebellum, the mossy fibres innervate not only the DCN but also the cerebellar granule cells. Burst stimulation applied to the mossy fibre–granule cell synapse resulted in long-term synaptic potentiation and an increase in intrinsic excitability, as shown by an NMDA receptor-dependent increase in the number of spikes evoked by a depolarizing test pulse, an increase in R_{input} and a decrease in spike threshold (Armano *et al.* 2000). A similar effect (increased spiking, reduced spike threshold) was also produced by burst stimulation applied to layer II/III glutamatergic inputs to layer V pyramidal neurones in a neocortical slice preparation (Sourdet *et al.* 2003). Such changes in intrinsic excitability may add computational flexibility to neuronal circuits.

Intrinsically bursting DCN neurones respond to EPSP bursts with one of two types of persistent change: either an increase in excitability manifested as an increase in evoked spike frequency, or a conversion from a bursting to a tonic firing pattern (Fig. 4*A*). Why do some intrinsically bursting DCN cells respond to EPSP bursts with a mode shift to tonic firing while others show a different response consisting of increasing the number of evoked spikes while retaining their previous burst-firing mode? One clue comes from a retrospective analysis showing that, in the basal state, mode-shifting cells responded to large positive current injections with smaller increases in firing rate (Fig. 4*E*). Another comes from the observation that the number of spikes evoked by EPSP bursts during the conditioning stimulation was similar between these two groups (data not shown). We suggest that mode-shifting and spike-increasing responses to EPSP bursts reflect a similar alteration of intrinsic conductances, merely superimposed upon two different baseline excitability profiles. A stringent test of this hypothesis will ultimately require identification of these conductances and their measurement with voltage-clamp recordings before and after EPSP bursts. K^+ and Ca^{2+}-sensitive K^+ conductances are particularly good candidates for mediating both excitability increases and mode-shifting.

While rapid, persistent synaptically driven changes in firing mode had not been previously reported, there is precedent for slower modulation of this parameter. In the stomatogastric ganglion of the spiny lobster *Panulirus* or the crab *Cancer,* identified neurones function in a circuit that generates gastric mill rhythms (Harris-Warrick, 2002). *In vivo*, these neurones are exposed to synaptic and neuromodulatory drive and they fire in bursts. When deprived of this input soon after being placed in culture, these neurones are mostly silent and respond to depolarizing current injection with tonic firing. However, after 2–4 days in culture (while still isolated from synaptic input), these neurones changed their activity from tonic firing to burst firing, thereby re-acquiring aspects of their *in vivo* firing pattern (Turrigiano *et al.* 1994). This involved upregulation of several inward currents including voltage-sensitive Ca^{2+} current, a rapidly inactivating voltage-sensitive Na^+ current and a slowly inactivating Na^+ plateau current, and downregulation of the transient K^+ current I_A and a delayed outward rectifier K^+ current (Turrigiano *et al.* 1995). At present, it is unclear whether the mechanisms engaged by this slow form of intrinsic plasticity will also be found in rapid changes in firing mode induced by EPSP bursts.

Ca^{2+} imaging experiments performed herein show that both EPSP bursts and IPSP bursts (and their consequent rebound spiking) produce large Ca^{2+} transients in the distal dendrite but these transients become smaller and slightly more prolonged (and hence subject to summation) in the soma (Figs 6 and 7). When these IPSP bursts were delivered to tonic firing DCN neurones, they produced essentially the same effect as EPSP bursts: an increase in average evoked firing rate and the set of changes which accompany this (reduced spike threshold, etc.). There is also precedent for driving persistent increases in intrinsic excitability by activating inhibitory synapses. In mouse brainstem slices, a 5 min long periodic stimulation of

GABAergic drive to neurones of the medial vestibular nucleus produced long-lasting increases in both the spontaneous firing rate and the increase in firing rate evoked by depolarizing current injection (Nelson *et al.* 2003). This phenomenon was associated with an increase in R_{input} and a decrease in the AHP following single spikes, but not with a change in spike threshold. It was mimicked and occluded by application of iberiotoxin, a specific blocker of large-conductance Ca^{2+}-dependent K^+ (BK) channels. Interestingly, this form of intrinsic excitability was not driven by rebound spiking and dendritic Ca^{2+} transients, as in the present case. Rather, it appeared to result from a reduction in basal Ca^{2+} concentration during the conditioning stimulus. Thus, there are at least two distinct mechanisms by which repeated activation of inhibitory GABAergic synapses can drive persistent increases in postsynaptic intrinsic excitability.

The observation that IPSP bursts followed by a brief pause are an ideal stimulus to evoke rebound spiking, associated dendritic Ca^{2+} transients, and ultimately, intrinsic plasticity of DCN neurones has potential implications for cerebellar circuit function. The inferior olive typically signals motor errors through spike firing that is conveyed to cerebellar Purkinje cells through excitatory climbing fibre input. Climbing fibre activation results in a transient acceleration in Purkinje cell firing rate followed by a brief pause (Armstrong *et al.* 1973; Eccles *et al.* 1974; Ruigrok, 1997). This will be conveyed via Purkinje cell axons to DCN neurones as an IPSP burst followed by a brief pause. Therefore, repeated activation of the inferior olive (as one might encounter in a motor learning task) might be able to persistently alter DCN intrinsic excitability through a climbing fibre–Purkinje cell disynaptic loop.

There are several caveats in interpreting the present experiments. We have referred to the stimulation delivered to the DCN by stimulating electrodes placed in the adjacent white matter in the presence of the $GABA_A$ antagonist picrotoxin as 'EPSP bursts'. However, the DCN also receive a number of extrinsic modulatory fibres including those utilizing the neurotransmitters acetylcholine (Woolf & Butcher, 1989), serotonin (Chan-Palay, 1976; Takeuchi *et al.* 1982; Kitzman & Bishop, 1994), noradrenaline (norepinephrine) (Olson & Fuxe, 1971; Eller & Chan-Palay, 1976) and histamine (Panula *et al.* 1989; Schwartz *et al.* 1991). DCN interneurones may also release glycine (Chen & Hillman, 1993; Rampon *et al.* 1996; Baurle & Grusser-Cornehls, 1997). $GABA_B$ receptors are unlikely to be activated by synaptic stimulation as previous work has shown $GABA_B$ antagonists to have no effects on evoked synaptic currents in DCN (Morishita & Sastry, 1995; Mouginot & Gähwiler, 1995). It is possible that the effects of 'EPSP bursts' on intrinsic plasticity may require the actions of neuromodulators. Similarly, 'IPSP bursts' in the presence of the ionotropic glutamate receptor antagonist kynurenate may also involve the release of modulatory neurotransmitters. In addition, the postsynaptic group I metabotropic glutamate receptors mGluR1 and mGluR5 are present in the DCN (Fotuhi *et al.* 1993; Romano *et al.* 1995). Since both our 'EPSP burst' and 'IPSP burst' protocols leave metabotropic glutamate receptors unblocked, it is possible that their activation also contributes to DCN intrinsic plasticity.

There is also a possibility that the persistent increases in intrinsic excitability produced by IPSP bursts reflect a persistent attenuation of tonic GABA release. Previous work has shown that under certain conditions IPSP bursts can give rise to LTD of *evoked* IPSPs recorded in the DCN (Aizenman *et al.* 1998). For this phenomenon to contribute to intrinsic plasticity, IPSP bursts would have to result in a sustained decrease of *tonic* GABAergic drive as well. While this is formally possible, we believe it is unlikely, as a similar form of intrinsic plasticity may be triggered by EPSP bursts in conditions where $GABA_A$ receptors are blocked.

A final caveat concerns the measurement of Ca^{2+} transients. We used the high-affinity dye Oregon Green BAPTA-1 (K_d *in vitro* = 170 nM) at a concentration of 200 μM. This is likely to introduce a high degree of Ca^{2+} chelation relative to the endogenous buffering capacity of the DCN neurone cytoplasm. In so doing, we may have produced a systematic slowing of both the rising and decay phases of the recorded evoked Ca^{2+} transients (Sabatini & Regehr, 1998). However, this would not be expected to differentially alter IPSP *versus* EPSP burst-evoked Ca^{2+} measurements or somatic *versus* dendritic measurements.

The present work extends our previous investigation into the modulation of intrinsic excitability of DCN neurones in two important aspects. Firstly, the modulation of the firing pattern of DCN neurones by EPSP bursts is a novel form of plasticity in this neurone. This phenomenon is particularly interesting from a computational point of view in that it might allow for plasticity in the neural representation of information by a spike timing code. Secondly, the discovery that physiologically pertinent patterns of IPSP bursts can cause a paradoxical increase in the excitability of DCN neurones suggests that the climbing fibre–Purkinje cell disynaptic loop may persistently alter DCN excitability. Further work to understand the signal transduction pathways involved in and the ion channels modulated during intrinsic excitability changes will be invaluable in understanding the role of such changes in phenomena such as information storage and signal integration.

References

Aizenman CD, Huang EJ & Linden DJ (2003). Morphological correlates of intrinsic electrical excitability in neurons of the deep cerebellar nuclei. *J Neurophysiol* **89**, 1738–1747.

Aizenman CD, Huang EJ, Manis PB & Linden DJ (2000). Use-dependent changes in synaptic strength at the Purkinje cell to deep nuclear synapse. *Prog Brain Res* **124**, 257–273.

Aizenman CD & Linden DJ (1999). Regulation of the rebound depolarization and spontaneous firing patterns of deep nuclear neurons in slices of rat cerebellum. *J Neurophysiol* **82**, 1697–1709.

Aizenman CD & Linden DJ (2000). Rapid, synaptically driven increases in the intrinsic excitability of cerebellar deep nuclear neurons. *Nature Neurosci* **3**, 109–111.

Aizenman CD, Manis PB & Linden DJ (1998). Polarity of long-term synaptic gain change is related to postsynaptic spike firing at a cerebellar inhibitory synapse. *Neuron* **21**, 827–835.

Armano S, Rossi P, Taglietti V & D'Angelo E (2000). Long-term potentiation of intrinsic excitability at the mossy fiber-granule cell synapse of rat cerebellum. *J Neurosci* **20**, 5208–5216.

Armstrong DM, Cogdell B & Harvey RJ (1973). Response of interpositus neurones to nerve stimulation in chloralose anesthetized cats. *Brain Res* **55**, 461–466.

Baurle J & Grusser-Cornehls U (1997). Differential number of glycine- and GABA-immunopositive neurons and terminals in the deep cerebellar nuclei of normal and Purkinje cell degeneration mutant mice. *J Comp Neurol* **382**, 443–458.

Chan-Palay V (1976). Serotonin axons in the supra- and subependymal plexuses and in the leptomeninges; their roles in local alterations of cerebrospinal fluid and vasomotor activity. *Brain Res* **102**, 103–130.

Chan-Palay V (1977). *Cerebellar Dentate Nucleus*. Springer-Verlag, Berlin.

Chen K, Aradi I, Thon N, Eghbal-Ahmadi M, Baram TZ & Soltesz I (2001). Persistently modified h-channels after complex febrile seizures convert the seizure-induced enhancement of inhibition to hyperexcitability. *Nature Med* **7**, 331–337.

Chen S & Hillman DE (1993). Colocalization of neurotransmitters in the deep cerebellar nuclei. *J Neurocytol* **22**, 81–91.

Eccles JC, Sabah NH & Taborikova H (1974). Excitatory and inhibitory responses of neurones of the cerebellar fastigial nucleus. *Exp Brain Res* **19**, 61–77.

Eller T & Chan-Palay V (1976). Afferents to the cerebellar lateral nucleus. Evidence from retrograde transport of horseradish peroxidase after pressure injections through micropipettes. *J Comp Neurol* **166**, 285–301.

Fotuhi M, Sharp AH, Glatt CE, Hwang PM, von Krosigk M, Snyder SH & Dawson TM (1993). Differential localization of phosphoinositide-linked metabotropic glutamate receptor (mGluR1) and the inositol 1,4,5-trisphosphate receptor in rat brain. *J Neurosci* **13**, 2001–2012.

Gauck V, Thomann M, Jaeger D & Borst A (2001). Spatial distribution of low- and high-voltage-activated calcium currents in neurons of the deep cerebellar nuclei. *J Neurosci* **21**, RC158.

Hansel C, Linden DJ & D'Angelo E (2001). Beyond parallel fiber LTD: the diversity of synaptic and non-synaptic plasticity in the cerebellum. *Nature Neuroscience* **4**, 467–475.

Harris-Warrick RM (2002). Voltage-sensitive ion channels in rhythmic motor systems. *Curr Opin Neurobiol* **12**, 646–651.

Jafri MS & Weinreich D (1998). Substance P regulates I_h via a NK-1 receptor in vagal sensory neurons of the ferret. *J Neurophysiol* **79**, 769–777.

Jahnsen H (1986). Electrophysiological characteristics of neurones in the guinea-pig deep cerebellar nuclei in vitro. *J Physiol* **372**, 129–147.

Kitzman PH & Bishop GA (1994). The origin of serotoninergic afferents to the cat's cerebellar nuclei. *J Comp Neurol* **340**, 541–550.

Lavond DG (2002). Role of the nuclei in eyeblink conditioning. *Ann N Y Acad Sci* **978**, 93–105.

LeDoux MS, Hurst DC & Lorden JF (1998). Single-unit activity of cerebellar nuclear cells in the awake genetically dystonic rat. *Neuroscience* **86**, 533–545.

Llinas R & Muhlethaler M (1988). Electrophysiology of guinea-pig cerebellar nuclear cells in the in vitro brain stem-cerebellar preparation. *J Physiol* **404**, 241–258.

McDevitt CJ, EbnerTJ & Bloedel JR (1987). Relationships between simultaneously recorded Purkinje cells and nuclear neurons. *Brain Res* **425**, 1–13.

Medina JF, Nores WL, Ohyama T & Mauk MD (2000). Mechanisms of cerebellar learning suggested by eyelid conditioning. *Curr Opin Neurobiol* **10**, 717–724.

Morishita W & Sastry BR (1995). Pharmacological characterization of pre- and postsynaptic $GABA_B$ receptors in the deep nuclei of rat cerebellar slices. *Neuroscience* **68**, 1127–1137.

Mouginot D & Gähwiler BH (1995). Characterization of synaptic connections between cortex and deep nuclei of the rat cerebellum in-vitro. *Neuroscience* **64**, 699–712.

Muri R & Knopfel T (1994). Activity induced elevations of intracellular calcium concentration in neurons of the deep cerebellar nuclei. *J Neurophysiol* **71**, 420–428.

Nelson AB, Krispel CM, Sekirnjak C & du Lac S (2003). Long-lasting increases in intrinsic excitability triggered by inhibition. *Neuron* **40**, 609–620.

Olson L & Fuxe K (1971). On the projections from the locus coeruleus noradrealine neurons: the cerebellar innervation. *Brain Res* **28**, 165–171.

Panula P, Pirvola U, Auvinen S & Airaksinen MS (1989). Histamine-immunoreactive nerve fibers in the rat brain. *Neuroscience* **28**, 585–610.

Poolos NP, Migliore M & Johnston D (2002). Pharmacological upregulation of h-channels reduces the excitability of pyramidal neuron dendrites. *Nat Neurosci* **5**, 767–774.

Raman IM, Gustafson AE & Padgett D (2000). Ionic currents and spontaneous firing in neurons isolated from the cerebellar nuclei. *J Neurosci* **20**, 9004–9016.

Rampon C, Luppi PH, Fort P, Peyron C & Jouvet M (1996). Distribution of glycine-immunoreactive cell bodies and fibers in the rat brain. *Neuroscience* **75**, 737–755.

Romano C, Sesma MA, McDonald CT, O'Malley K, Van den Pol AN & Olney JW (1995). Distribution of metabotropic glutamate receptor mGluR5 immunoreactivity in rat brain. *J Comp Neurol* **355**, 455–469.

Ruigrok TJ (1997). Cerebellar nuclei: the olivary connection. *Prog Brain Res* **114**, 167–192.

Sabatini BL & Regehr WG (1998). Optical measurement of presynaptic calcium currents. *Biophys J* **74**, 1549–1563.

Schwartz JC, Arrang JM, Garbarg M, Pollard H & Ruat M (1991). Histaminergic transmission in the mammalian brain. *Physiol Rev* **71**, 1–51.

Sourdet V, Russier M, Daoudal G, Ankri N & Debanne D (2003). Long-term enhancement of neuronal excitability and temporal fidelity mediated by metabotropic glutamate receptor subtype 5. *J Neurosci* **23**, 10238–10248.

Storm JF (1990). Potassium currents in hippocampal pyramidal cells. *Prog Brain Res* **83**, 161–187.

Takeuchi Y, Kimura H & Sano Y (1982). Immunohistochemical demonstration of serotonin-containing nerve fibers in the cerebellum. *Cell Tissue Res* **226**, 1–12.

Thach WT (1968). Discharge of Purkinje and cerebellar nuclear neurons during rapidly alternating arm movements in the monkey. *J Neurophysiol* **31**, 785–797.

Turrigiano G, Abbott LF & Marder E (1994). Activity-dependent changes in the intrinsic-properties of cultured neurons. *Science* **264**, 974–977.

Turrigiano G, LeMasson G & Marder E (1995). Selective regulation of current densities underlies spontaneous changes in the activity of cultured neurons. *J Neurosci* **15**, 3640–3652.

Williams SR, Christensen SR, Stuart GJ & Hausser M (2002). Membrane potential bistability is controlled by the hyperpolarization-activated current I_H in rat cerebellar Purkinje neurons in vitro. *J Physiol* **539**, 469–483.

Woolf NJ & Butcher LL (1989). Cholinergic systems in the rat brain. IV. Descending projections of the pontomesencephalic tegmentum. *Brain Res Bull* **23**, 519–540.

Zhang W & Linden DJ (2003). The other side of the engram: experience-driven changes in neuronal intrinsic excitability. *Nat Rev Neurosci* **4**, 885–900.

Acknowledgements

Thanks to Hiroshi Nishiyama, Andrei Sdrulla, Ying Shen and Sang Jeong Kim for helpful suggestions and to Roland Bock for technical support. This work was supported by USPHS MH51106, MH01590, MH61974 and the Develbiss Fund.

Supplementary material

The online version of this paper can be accessed at: DOI: 10.1113/jphysiol.2004.071696
http://jp.physoc.org/cgi/content/full/jphysiol.2004.071696/DC1 and contains the following supplementary material:

Supplementary Figure 1. Increases in intrinsic excitability evoked by EPSP or IPSP bursts are uncorrelated with increases in input resistance.

Supplementary Figure 2. Blockade of excitability increase by BAPTA is not due to saturation of neuronal excitability.

This material can also be found at:
http://www.blackwellpublishing.com/products/journals/suppmat/tjp/tjp602/tjp602sm.htm